Nuclear Engineering and Technology 53 (2021) 3359–3366

Contents lists available at ScienceDirect

Nuclear Engineering and Technology

journal homepage: www.elsevier.com/locate/net

Original Article

Thermal conductivity prediction model for compacted bentonites considering temperature variations

Seok Yoon [a,*], Min-Jun Kim [b], Seunghun Park [c], Geon-Young Kim [a]

[a] Radioactive Waste Disposal Research Division, KAERI, Daejeon, 34057, South Korea
[b] Deep Subsurface Research Center, KIGAM, Daejeon, 34132, South Korea
[c] Department of Energy Resource Engineering, Inha University, Incheon, 22212, South Korea

ARTICLE INFO

Article history:
Received 7 February 2021
Received in revised form
29 March 2021
Accepted 1 May 2021
Available online 14 May 2021

Keywords:
Compacted bentonite
Thermal conductivity
Temperature variation
Multiple regression analysis
Metamodel

ABSTRACT

An engineered barrier system (EBS) for the deep geological disposal of high-level radioactive waste (HLW) is composed of a disposal canister, buffer material, gap-filling material, and backfill material. As the buffer fills the empty space between the disposal canisters and the near-field rock mass, heat energy from the canisters is released to the surrounding buffer material. It is vital that this heat energy is rapidly dissipated to the near-field rock mass, and thus the thermal conductivity of the buffer is a key parameter to consider when evaluating the safety of the overall disposal system. Therefore, to take into consideration the sizeable amount of heat being released from such canisters, this study investigated the thermal conductivity of Korean compacted bentonites and its variation within a temperature range of 25 °C to 80−90 °C. As a result, thermal conductivity increased by 5−20% as the temperature increased. Furthermore, temperature had a greater effect under higher degrees of saturation and a lower impact under higher dry densities. This study also conducted a regression analysis with 147 sets of data to estimate the thermal conductivity of the compacted bentonite considering the initial dry density, water content, and variations in temperature. Furthermore, the Kriging method was adopted to establish an uncertainty metamodel of thermal conductivity to verify the regression model. The R^2 value of the regression model was 0.925, and the regression model and metamodel showed similar results.

1. Introduction

Spent fuel can be deemed as high-level radioactive waste (HLW) with extremely high radiation levels; hence, it must be safely disposed of using the deep geological method [1]. An engineered barrier system (EBS), which was developed to safely dispose of HLW, is composed of a disposal canister, buffer material, backfill material, and gap-filling material (Fig. 1). The buffer material fills the empty space between the container and the near-field rock mass, protecting the disposal container by minimizing physical impacts and the penetration of groundwater from the near-field rock mass [2–4]. Additionally, the buffer material also has the role of rapidly releasing the heat generated by decay in the disposal container to the surrounding buffer material. Decay heat must be propagated to prevent heat from accumulating in the canister, which can potentially compromise the overall safety of the EBS [2,5]. Bentonite clay mineral, which is composed of montmorillonite, has been reported by several researchers as the most suitable buffer material since it meets all performance requirements [3,6,7]. Bentonite has a structure consisting of bonded aluminum octahedral layers and silicon tetrahedral layers. This structure enables isomorphous substitution, in which aluminum is replaced with magnesium or iron [8,9]. According to the exchangeable cations between the layers, bentonite clay can be largely divided into Na-type bentonite and Ca-type bentonite. In Korea, Ca-type bentonite is produced in the Gyeongju area.

As the dry density of a bentonite buffer should be greater than 1.6 g/cm^3 [2,7], buffers are installed as compacted blocks that are produced by compressing bentonite powder. A bentonite buffer must meet several requirements to achieve an acceptable level of performance. For example, the specific heat capacity and thermal conductivity of the bentonite buffer are key factors that impact the overall performance of an EBS. Specifically, thermal conductivity is a key parameter that determines the maximum temperature of the buffer material as it controls the transfer rate of decay heat [10]. For this reason, there has been a multitude of research on the thermal

* Corresponding author.
E-mail address: syoon@kaeri.re.kr (S. Yoon).

https://doi.org/10.1016/j.net.2021.05.001

Nomenclature

A	correlation matrix
F	regression function
H	probe constant
I	heating current (A)
K	probe constant
R	electric resistance of the probe per unit length (Ω/m)
S	degree of saturation
T	temperature (°C)
n	number of design variables
t	time (s)
z	random error

Greek letters

γ_d	dry density ($g \cdot cm^{-3}$)
λ	thermal conductivity (W/(m·K))
ω	water content
θ	unknown smoothing parameter

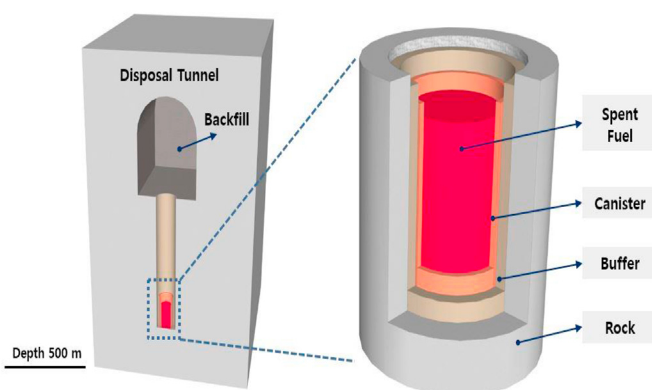

Fig. 1. Components of an engineered barrier system [2].

conductivity of compacted bentonites [2,10–13]. Recently, Zhou et al. (2021) [14] presented a mathematical model for three-layer media such as bentonite blocks, bentonite pellets, and near-field rock-mass in nuclear waste repositories. However, the majority of studies focus on a limited number of factors, such as dry density and saturation. In real-world disposal environments, large amounts of heat are emitted from the disposal canister and subsequently transferred to the bentonite buffer. In addition, groundwater that penetrates from the intact rock-mass increases the water content of the bentonite buffer. Therefore, it is necessary to comprehensively consider both the saturation and the temperature of the buffer. During the initial stages of disposal, heat from the disposal canister causes the bentonite buffer to decrease in saturation [2]. However, the buffer may be subsequently saturated by groundwater depending on its hydraulic conductivity, pore pressure, and thermal gradient. The saturation of the buffer is maintained at constant levels, even though high-temperature heat is continuously transferred to the buffer [15]. Despite this importance, there are few studies that investigate the thermal conductivity of bentonite buffers and its variation with temperature changes, and a thermal conductivity model that considers temperature has yet to be developed. Xu et al. (2019) [16] experimentally investigated MX-80 and GMZ bentonite to determine how thermal conductivity varies according to increasing temperature. The results determined that the thermal conductivity of compacted bentonites increased more rapidly with temperature for samples with higher water content. Therefore, overall safety evaluations of EBSs require thermal conductivity behavior models of compacted bentonites that consider changes in thermal conductivity according to temperature changes. Whereas several thermal conductivity model equations that consider water content or dry density have been introduced for bentonite [2,12,17,18], a thermal conductivity behavior model that also considers temperature has yet to be proposed.

Therefore, this research experimentally investigated the thermal conductivity of a Korean compacted bentonite for temperatures ranging from 25 °C to 80–90 °C. In addition, a thermal conductivity model that considers dry density, water content, and temperature was proposed through regression analysis. Furthermore, a meta-analysis was also conducted to verify the regression model.

2. Test setup

2.1. Materials and test equipment

In this research, the thermal conductivity of Gyeongju (KJ) compacted bentonite was measured. Using the USCS (unified soil classification system) method, KJ bentonite powder is classified as CH, which refers to a highly plastic clay [8]. The chemical composition is primarily Al_2O_3 and SiO_2, and the composition ratio of CaO is 5–6 times higher than that of Na_2O [19]. Furthermore, KJ bentonite contains 62–65% montmorillonite, as reported in a previous research on its detailed basic properties [19]. The KJ bentonite powder was compacted in a steel mold using a hydraulic press to achieve a target density. The sample shape for the thermal conductivity test was a cuboid form with dimensions of 100 mm × 50 mm × 20 mm [20].

The QTM (Quick thermal conductivity meter)-500 equipment, which is based on the transient hot wire theory to measure thermal conductivity as shown in Eq. (1), was used to measure the thermal conductivity of the Korean compacted bentonite. This equipment uses the heating time and relative temperature increase between heated wires when a certain amount of heat is applied to the wires [21].

$$\lambda = K \cdot R \cdot I^2 \cdot \ln(t_2 / t_1) \Big/ (T_2 - T_1) - H \quad (1)$$

where λ is the thermal conductivity (W/(m·K)), I is the current (A), t_1 and t_2 represent measurement time (s), and T_1 and T_2 represent the temperature (K) at times t_1 and t_2. Furthermore, K and H indicate the probe constants, which should be calculated from reference samples with pre-obtained thermal conductivity values. Styrofoam (0.036 W/(m·K)), silicon rubber (0.24 W/(m·K)), and quartz (1.42 W/(m·K)) were used as reference samples. Table 1 shows the specifications of QTM-500 [20]. The precision and reproducibility of the QTM-500 equipment is ±5% and ±3%, respectively [20].

Table 1
Specifications of QTM-500 [20].

Note	Specification (QTM-500 equipment)
Measuring method	Hot wire method
Precision	±5%
Reproducibility	±3%
Temperature	−10–200 °C
Heater current precision	±0.05%
Measuring time	Standard 60 s

2.2. Test process

The thermal conductivity of the bentonite specimen was measured according to temperature. The bentonite sample and the QTM-500 probe were completely sealed with heat resistant tape and silicon to prevent water from escaping out of the bentonite sample. Both the sample and probe were subsequently place in a convection oven to adjust the temperature (Fig. 2). A temperature sensor was also inserted into another bentonite sample under the same conditions to measure the temperature of the bentonite (this sample was not used in the test). After setting the temperature of the convection oven, as shown in Fig. 3, equilibrium was achieved after approximately 300–400 min. For the test at room temperature, the convection oven was set to 25 °C. The thermal conductivity of the compacted bentonite was measured when the temperature of the bentonite reached a steady state condition. Fig. 4 summarizes the test process to measure the thermal conductivity of the compacted bentonite sample considering temperature increases.

3. Results and discussion

3.1. Test results

Although the dry density of a buffer material should be at least 1.6 g/cm^3 to satisfy performance requirements [22,23], variations in thermal conductivity according to water content and temperature were measured under dry density conditions between 1.31 g/cm^3 ~ 1.84 g/cm^3 to investigate temperature effects under various dry density and water content conditions. As shown in Fig. 5, the thermal conductivity of the compacted bentonite increases with increasing temperature, increasing by approximately 4–20% compared to the thermal conductivity value at 25 °C. The results show that higher water content values result in greater increases in thermal conductivity, which is believed to be due to the heat transfer by latent heat [16]. Soils are composed of three phases: water, air, and solid particles such as clay particles. It is known that the thermal conductivity of a soil increases with temperature [24]: as the temperature increases, water islands [16,24] are formed by the increased movement of water vapor due to the menisci of water in the bentonite.

In addition, the thermal conductivity was measured at various temperatures for compacted bentonite with different dry densities under controlled water content conditions. As a result, the thermal conductivity of the compacted bentonite was found to increase as temperature rises, although the thermal conductivity generally increased by a lesser degree for samples with higher dry densities. This is believed to be due to the greater proportion of space in the soil taken up by air in samples with lower dry densities, resulting in latent heat transfer due to pure air movement, which causes the thermal conductivity to increase. The sample weight was also measured according to a rise in temperature under confined conditions, where the sample volume was assumed to be constant. As a

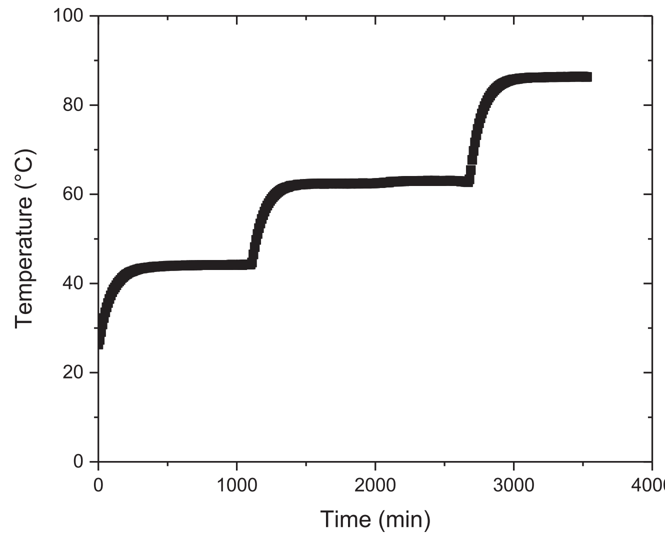

Fig. 3. Temperature increase during the test.

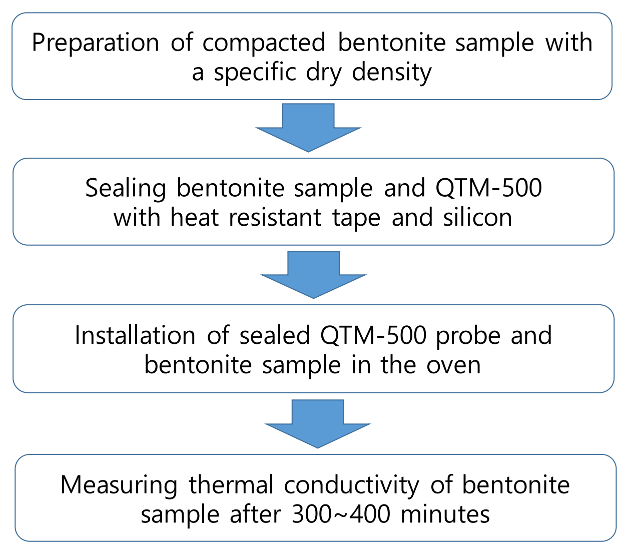

Fig. 4. Test process for measuring thermal conductivity.

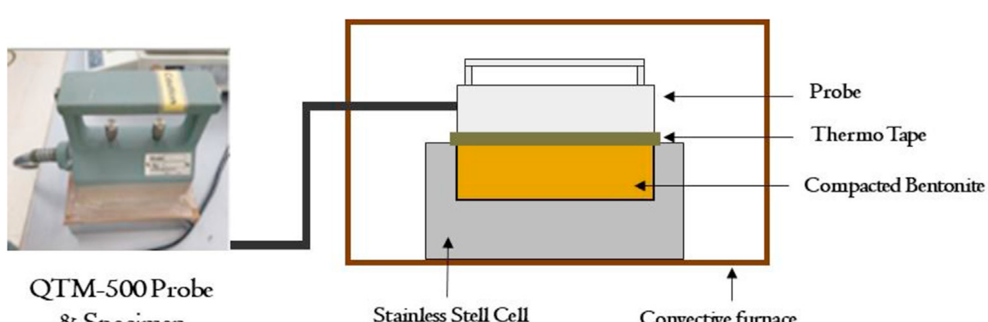

Fig. 2. Experimental apparatus for the thermal conductivity measurement test.

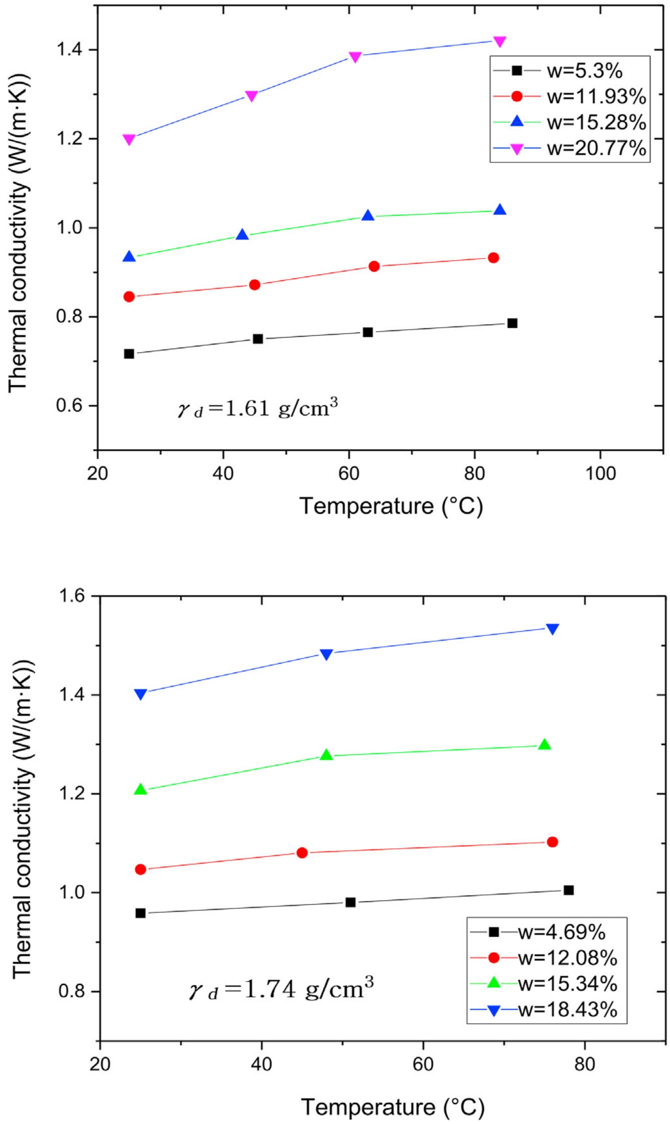

Fig. 5. Thermal conductivity with respect to increasing temperature.

result, the sample weight slightly decreased as the temperature rose, which is believed to be due to a decrease in the mass of water according to temperature as the pore water density decreased. Fig. 6 shows the changes in water density according to temperature proposed by a previous research [25] in addition to the changes in pore water density as experimentally derived by the present study. The decreased sample weight is thought to be due to the decreased water mass, which is converted to water density with respect to temperature. The dry density of the sample was 1.61 g/cm^3, and initial water content was 11.93%. As shown in Fig. 6, the results of both cases are almost identical. In the present study, the mass balance used to measure the sample mass under confined conditions was placed in the convection oven with the sample, at which the sample temperature and mass were measured.

Xu et al. (2019) [16] reported similar experimental results for Na-type bentonite, with thermal conductivity increasing with temperature to a greater degree under higher water content and lower dry density conditions.

Furthermore, thermal conductivity was measured according to increasing temperature under dry conditions. Fig. 7 shows the thermal conductivity variation of compacted bentonite samples

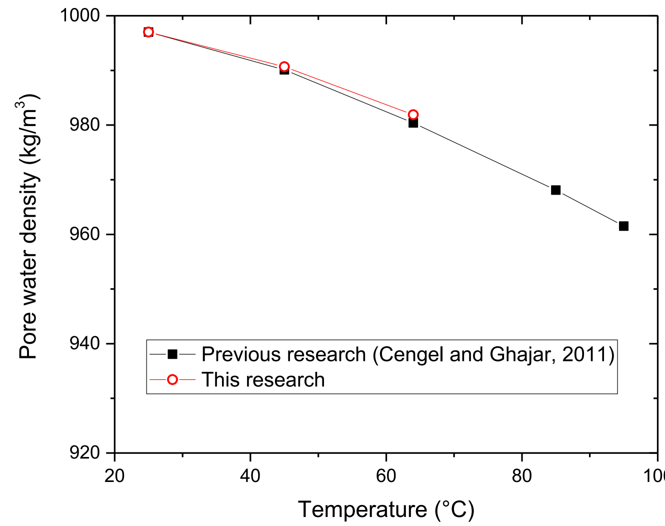

Fig. 6. Water density with respect to increasing temperature.

with various dry densities under dry conditions; the increase in thermal conductivity was approximately 4–10% higher in the 80–90 °C range than at room temperature. This is because water is not present in dry conditions, and thus water islands are not formed by the movement of steam. Consequently, the increase in thermal conductivity due to the clay particles and air is smaller than when water is present. In particular, less heat is transferred by air movement as the dry density increases. For this reason, the increase in thermal conductivity with increasing temperature is miniscule. FEBEX bentonite also exhibited a linear increase in thermal conductivity of approximately 3–4% from 20–30 °C to 80–90 °C [1,26].

Fig. 8 shows the thermal conductivity test results of the compacted bentonite samples and the change in thermal conductivity of water [25]. The results were deduced with the dry density of the compacted bentonite as 1.61 g/cm^3, and the initial water contents were 0 and 11.93%. The results show that the thermal conductivities of the clay particles, water, and air increases with increasing temperature. However, the thermal conductivity of water is known to increase at a decreased rate as temperature rises, ultimately

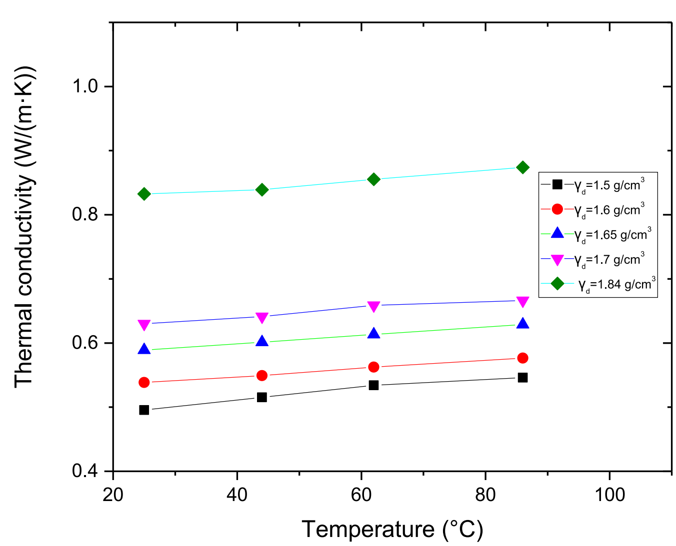

Fig. 7. Thermal conductivity variation under dry conditions.

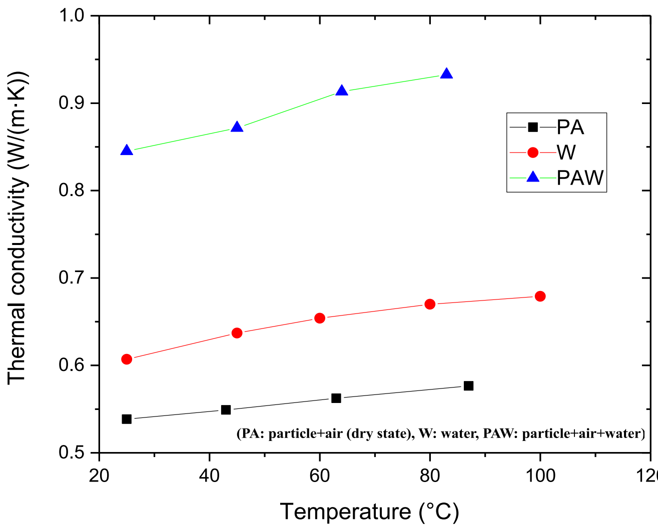

Fig. 8. Summary of the thermal conductivity variations with respect to increasing temperature.

resulting in the thermal conductivity decreasing beyond 120 °C [25]. As such, whereas the thermal conductivity of compacted bentonite under dry conditions linearly increases within the temperature range from 25 °C to 80–90 °C, the rate of increase of thermal conductivity under the three-phase condition is slightly lower within the same temperature range.

3.2. Multiple regression analysis

In this section, an empirical model is suggested to predict thermal conductivity for compacted bentonite with 39 experimental data sets involving Ca-type bentonite from a previous study [23] and 108 data sets from the experiments conducted in this study. All data sets were obtained using the QTM-500 equipment, and all specimens comprised of the same Ca-type bentonite with a compacted shape. Table 2 shows basic statistical quantities of the 147 data sets.

As the dependent variable must follow a normal distribution [27], it was verified using a P–P plot module of the SPSS (Statistical Package for the Social Sciences) software. The dependent variable satisfies a normal distribution due to the fact that most data follow linearity [23]. Multiple regression analysis was performed with initial water content, initial dry density, and temperature as independent variables, and thermal conductivity as the dependent variable. Five outliers among the 147 data sets were excluded in the regression analysis. As thermal conductivity showed a nonlinear increase with increasing temperature, it was converted to a logarithmic scale. Eq. (2) represents the multiple regression equation:

$$\lambda = -1.198 + 2.628\omega + 1.055\gamma_d + 0.030\ \ln(T) \tag{2}$$

where ω is the water content, γ_d is the dry density (g/cm^3), and T is the temperature (°C). By considering the decrease in water content shown in Fig. 6, which is due to the decrease in pore water as the temperatures rises, Eq. (2) can be modified to Eq. (3).

$$\lambda = -1.211 + 2.648\omega + 1.054\gamma_d + 0.034\ \ln(T) \tag{3}$$

As both Eq. (2) and Eq. (3) have relative errors within 0.2%, this indicates that the decrease in the sample water content due to the increased temperature was negligible.

Table 3 shows the multiple regression analysis results. Based on a *t*-test, the P-values for the three independent variables were less than 0.01, indicating that the three independent variables can be statistically selected to predict thermal conductivity [28]. The P-value represents the probability that the test statistic of the observed data supports the null hypothesis, which assumes that the independent variable does not affect the dependent variable [27]. In addition, the variance inflation factor (VIF) was significantly less than 10, indicating that there was no correlation among the independent variables [27,28], which is important for regression analysis [28]. The coefficient of determination (R^2), which is the regression sum of squares divided by the total sum of squares, and the adjusted coefficient of determination ($_{adj}R^2$) were 0.924 and 0.925, respectively.

An analysis of variance, also referred to as ANOVA, should be performed to support the significance of the regression analysis [27–29]. In ANOVA, the degree of freedom and sum of squares can be used to obtain an F-value [23], which can be defined as the mean regression sum of squares divided by the mean squared error [28]. Table 4 represents the ANOVA results. As the P-value was less than 0.01, it is thought that the independent variables can affect the dependent variable.

A residual analysis should also be performed to support the statistical assumption of the regression equation [19,28]. Residuals refer to the differences between the measured and predicted values of thermal conductivity. In particular, residuals should follow the normality and homoscedasticity condition in regression analysis. The normal distribution condition for the residual analysis can be investigated based on kurtosis and skewness values as well as the P-values of the Shapiro–Wilk and Kolmogorov–Smirnov tests [30]. Since the kurtosis and skewness values, which were −0.267 and 0.550, respectively, were less than 2, it can be thought that the residuals follow a normal distribution condition [27]. The Shapiro–Wilk test is used to investigate the normal distribution condition for small sample sizes less than 2000 [30]. If the P-value of the Shapiro–Wilk test for standardized residuals is larger than 0.05, the residuals satisfy a normal distribution condition [19]. In

Table 3
Multiple regression analysis results.

	B	Standard error	t	P-value	VIF
Constant	−1.198	0.081	−14.727	<0.01	
X1 (water content)	2.628	0.073	36.021	<0.01	1.028
X2 (dry density)	1.055	0.041	25.966	<0.01	1.054
X3 (temperature)	0.030	0.010	3.059	<0.01	1.026
R^2	0.925				
$_{adj}R^2$	0.924				

B: non-standardized coefficient, *t*: *B*/standard error, *VIF*: variance inflation factor.

Table 2
Statistical quantities of the 147 data sets.

	N	Minimum	Maximum	Average	Standard deviation	Skewness	Kurtosis
Water content	147	0	0.234	0.072	0.067	0.401	−1.055
Dry density (g/cm^3)		1.314	1.836	1.636	0.116	−0.767	0.781
Temperature (°C)		25	87	44.847	22.204	0.634	−1.086
Thermal conductivity (W/(m·K))		0.388	1.536	0.834	0.227	0.767	0.661

Table 4
ANOVA results.

	DF	SS	MS	F	P-value
Regression	3	5.151	1.717	570.144	<0.01
Residuals	138	0.416	0.003		
Total	141	5.567			

this analysis, the P-value based on the Shapiro–Wilk test was 0.963. Additionally, the residuals should follow the homoscedasticity condition to use the regression equation, which is determined by plotting standardized residuals in disorder within a range of ±3 [31]. In this analysis, the residuals satisfy the homoscedasticity condition due to the absence of a specific regular distribution [32].

3.3. Metamodel

An accurate mathematical model is often difficult to obtain due to the uncertainty involved. As described in the previous section, thermal conductivity of compacted bentonite also has uncertainty, exhibiting a nonlinear tendency with regard to temperature variation. Thus, as a means of improving the accuracy of predicting the target value, this study presents a metamodel that serves as a simplified approximation of the actual, complicated model. Referred to as a 'model of a model' or a surrogate model, metamodeling techniques are frequently employed across the engineering disciplines in conjunction with complicated simulation models or physical experiments [33]. Representative techniques for metamodeling comprise of polynomial response surfaces, neural networks, and the Kriging model [34]. In this study, the Kriging model was employed as a metamodel as it is an optimal Gaussian interpolation process based on the regression analysis of complicated computational simulations and is weighted depending on spatial covariance values [35]. Furthermore, as the Kriging model is also known as a suitable approximation for highly nonlinear functions [36], this method was selected to estimate thermal conductivity in this study. The ordinary Kriging model is represented as the summation of a regression model and a stochastic process, representing an unknown function y(x), as formulated in Ref. [5]:

$$y(x) = \sum_{j=0}^{L} \beta_j \cdot B_j(x) + z(x) \tag{4}$$

where β_j is the unknown coefficient of function $B_j(x)$ where j = 1, 2 … L is a selected basis over the experimental domain, and z(x) indicates the random error.

The Gaussian correlation function $r(\theta; s, t)$ with zero mean and variance σ^2 can be employed to calculate the random error in the Kriging model, as follows:

$$r(\theta; s, t) = Corr(z(s), z(t)) = \exp\left\{ -\sum_{k=1}^{n} \theta_k |s_k - t_k|^2 \right\} \tag{5}$$

where θ_k is an unknown smoothing parameter, n indicates the number of input factors, and s_k and t_k are kth components of the samples. Predicted Kriging estimates, $\widehat{y}(x)$, of the response *y(x)* for untried values of *x* can be represented as:

$$\widehat{y}(x) = b(x)\widehat{\beta} + r'(x)A^{-1}(\theta)(y - B\widehat{\beta}) \tag{6}$$

where *A* represents the correlation matrix and $r'(x) = \{r(\theta; x_1, x), \ldots, r(\theta; x_n, x)\}'$. When it comes to the Gaussian process, the likelihood is defined by a function b(x) (with variance σ^2) and correlation parameters. In this case, the maximum likelihood estimator of σ can be obtained as follows:

$$\widehat{\sigma}^2 = (y - F\tilde{\beta})R^{-1}(y - F\widehat{\beta}) \Big/ n_s \tag{7}$$

where *F* is the regression function and n_s is the number of samples.

The Kriging method was conducted by running the MATLAB code that was developed in Ref. [37]. Among the total 147 data sets of the experimental results, 50 data sets were used to develop the Kriging metamodel, whereas the remaining 97 data sets were tested to validate the constructed metamodel. Table 5 presents the constants of the metamodel with regard to each dependent variable.

Using the metamodel with the obtained coefficients, thermal conductivity was estimated for the 97 data sets with the same independent variables as the validation data sets. The estimated thermal conductivity values were then compared with the experimental data to analyze the accuracy of the metamodel. Relative error analysis was initially conducted, which resulted in the metamodel exhibiting an average relative error of 5.77%. In addition, the independent-samples *t*-test, with the assumption of equal variance, was performed to investigate the significant differences between the experimental results and the estimated values [38]. As a result, the significant probability (P-value) was determined as 0.69 (Table 6). As this value exceeds the significance level of 0.05, it can be said that there is no statistical significance, which represents the difference between the experimental data and the predicted values.

The results of the uncertainty analysis indicate that the established Kriging metamodel is a highly reliable means of predicting the thermal conductivity of compacted bentonite with respect to unknown water content, dry density, and temperature. Fig. 9 shows the thermal conductivity values that were obtained using the metamodel and the regression model with respect to the original experimental data sets, which clearly shows the lack of significant differences between the metamodel and the regression model.

4. Conclusion

In actual radioactive waste disposal environments, bentonite buffers undergo a complex phenomenon involving temperature and saturation changes. This is due to the large amounts of heat released from the disposal container and the groundwater inflow from the intact rock. Therefore, it is necessary to investigate the physical properties of bentonite that are affected by changes in buffer temperature and saturation. For this purpose, this study investigated changes in thermal conductivity considering temperature change and water content.

Firstly, the thermal conductivity of compacted bentonite was measured under various water content conditions at temperatures ranging from room temperature to 80–90 °C. To measure the change in thermal conductivity with temperature, the samples were placed in a convection oven. At the 80–90 °C range, the thermal conductivity of the compacted bentonite was approximately 10–20% higher than the thermal conductivity at room temperature. In addition, the value of thermal conductivity increased with water content. Furthermore, the thermal conductivity of compacted bentonite at different temperatures was obtained for various dry densities under controlled water content conditions and in a dry state. As a result, thermal conductivity

Table 5
Constants of the metamodels based on Gaussian Kriging theory.

	Mean	Variance	Water content	Dry density	Temperature
Coefficients	0.8942	0.071	9.405E+01	3.602E+02	1.355E-04

Table 6
Result of the statistical T-test.

	Mean	Variance	Pooled variance	Degree of freedom	P-value (2-tailed)
Experiment data	0.8420	0.0494	0.0482	192	0.6985
Predicted data	0.8542	0.0471			

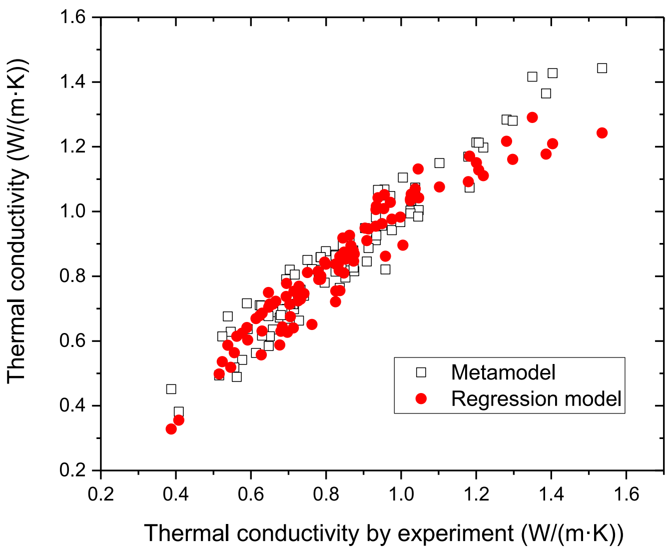

Fig. 9. Thermal conductivity according to the metamodel and the regression model.

increased to a lesser degree according to temperature as dry density increased, and to an even lesser degree in a dry state.

Using the 108 data sets derived from this study in addition to 39 data sets from a previous study that used the same sample specimen, a multiple regression analysis was performed using a total of 147 data sets to propose a thermal conductivity model for compacted bentonite. The independent variables were initial saturation, initial dry density, and temperature, and the temperature range for the test was from room temperature to 80–90 °C. The multiple regression analysis resulted in a relatively high R^2 value of 0.925, and all statistical significances of the multiple regression analysis were satisfied. Furthermore, the regression model was compared with the metamodel, and the results between the metamodel and the regression model were highly similar. Therefore, the regression equation proposed in this study can be used as key input data in future disposal site stability analysis tasks.

In addition, under actual medium-to-long-term disposal conditions, the saturation of the bentonite buffer continuously increases despite the emission of heat from the disposal canister due to the infiltration of groundwater from the intact rock. This leads to an increase in the thermal conductivity of the compacted bentonite. The test results obtained in this study are expected to be used as a significant resource when evaluating the integrity of bentonite buffers under medium-to-long-term disposal conditions. Further, the results could be useful in disposal site design processes and engineering barrier system performance evaluations that aim to increase the maximum temperature and decrease the disposal area.

Declaration of competing interest

The authors declare that they have no known competing financial interests or personal relationships that could have appeared to influence the work reported in this paper.

Acknowledgements

This research was funded by the Basic Research Project (2020R1F1A1072379) and Nuclear Research and Development Program (2021M2E3A2041351) by the National Research Foundation of Korea.

References

[1] M.V. Villar, Thermo-hydro-mechanical characterization and process in the clay barrier of a high level radioactive waste repository. State of the Art Report, Informes Técnicos Ciemat 1044 (2004). Octubre.
[2] S. Park, S. Yoon, S. Kwon, G.Y. Kim, A prediction of saturated conductivity for compacted bentonite buffer in a high-level radioactive waste disposal system, J. Nucl. Fuel Cycle Waste Technol. 18 (2) (2020) 133–141.
[3] J. Nilsson, Field compaction of bentonite-sand backfilling, Eng. Geol. 21 (1985) 367–376.
[4] W.J. Cho, Bentonite Barrier Material for Radioactive Waste Disposal, 2019. KAERI/GP-535.
[5] M.J. Kim, S.R. Lee, S. Yoon, M.S. Kim, Optimal initial condition of a bentonite buffer with regard to thermal behavior in a high-level radioactive waste repository, Comput. Geotech. 104 (2018) 109–117.
[6] T. Kanno, T. Fujita, S. Takeuchi, H. Ishikawa, K. Hara, M. Nakano, Coupled thermos-hydro mechanical modelling of bentonite buffer material, Int. J. Numer. Anal. Methods GeoMech. 23 (1999) 1281–1307.
[7] S.G. Zihms, J.F. Harriongton, Thermal cycling: impact on bentonite permeability, Mineral. Mag. 79 (6) (2015) 1543–1550.
[8] B.M. Das, Principle of Geotechnical Engineering, sixth ed. Nelson, 2006.
[9] J.K. Mitchell, K. Soga, Fundamentals of Soil Behavior, third ed., John Wiley & Sons Inc., New York, 2005.
[10] S. Knutsson, On the Thermal Conductivity and Thermal Diffusivity of Highly Compacted Bentonite, 1983. SKB Technical Report 83-72.
[11] H.T. Bang, S. Yoon, H. Jeon, Application of machine learning methods to predict a thermal conductivity model for compacted bentonite, Ann. Nucl. Energy 142 (2020) 107395.
[12] JNC, H12 Project to Establish Technical Basis for HLW Disposal in Japan (Supporting Report 2), JNC TN1400 99-020, Japan Nuclear Cycle Development Institute, 1999.
[13] M. Wang, Y.F. Chen, S. Zhou, R. Hu, C.B. Zhou, A homogenization-based model for the effective thermal conductivity of bentonite-sand-based buffer material, Int. Commun. Heat Mass Tran. 68 (2015) 43–49.
[14] X. Zhou, D. Sun, Y. Xu, A new thermal analysis model with three heat conduction layers in the nuclear waste repository, Nucl. Eng. Des. 371 (2021) 110929.
[15] N. Sultan, P. Delage, Y.J. Cui, Temperature effects on the volume change behavior of Boom clay, Eng. Geol. 64 (2002) 135–145.
[16] Y. Xu, D. Sun, Z. Zeng, H. Lv, Temperature dependence of apparent thermal conductivity of compacted bentonite as buffer material for high-level radioactive waste repository, Appl. Clay Sci. 174 (2019) 10–14.
[17] W.Z. Chen, Y.S. Ma, H.D. Yu, F.F. Li, X.L. Li, X. Sillen, Effects of temperature and thermally-induced microstructure change on hydraulic conductivity of Boom clay, J. Rock Mech. Geotech. Eng. 9 (2018) 383–395.
[18] J.W. Lee, H.J. Choi, J.Y. Lee, Thermal conductivity of compacted bentonite as a buffer material for a high-level radioactive waste repository, Ann. Nucl. Energy 94 (2016) 848–855.
[19] S. Yoon, J.S. Jeon, G.Y. Kim, J.H. Seong, M.H. Baik, Specific heat capacity model for compacted bentonite buffer materials, Ann. Nucl. Energy 125 (2019) 18–25.
[20] QTM Thermal Conductivity Meter QTM-500 Operation Manual, Ver.08 98-595-0009..
[21] M.S. Lee, H.J. Choi, J.O. Lee, J.P. Lee, Improvement of the Thermal Conductivity of a Compact Bentonite Buffer, 2013. KAERI/TR-5311/2013.
[22] W.J. Cho, G.Y. Kim, Reconsideration of thermal criteria for Korean spent fuel repository, Ann. Nucl. Energy 88 (2016) 73–82.
[23] S. Yoon, W. Cho, C. Lee, G.Y. Kim, Thermal conductivity of Korean compacted bentonite buffer materials for a nuclear waste repository, Energies 11 (2018) 2269.
[24] J.R. Phillip, D.A.D. Vries, Moisture movement in porous materials under temperature gradients, Trans. Am. Geophys. Union 38 (1957) 222–232.
[25] Y.A. Cengel, A.J. Ghajar, Heat and Mass Transfer: Fundamentals and Applications, fourth ed., McGraw Hill Education, 2011.
[26] A. Beziat, M. Dardaine, V. Gabis, Effect of compaction pressure and water

content on the thermal conductivity of some natural clays, Clay Clay Miner. 36 (5) (1988) 462–466.
[27] I.H. Lee, Easy Flow Regression Analysis, Hannarae Publishing Corporation, 2014.
[28] J.Y. Park, Statistical Entrainment Growth Rate Estimation Model for Debris-Flow Runout Prediction, Master Thesis, KAIST, 2015.
[29] Data Solution Consulting Team, SPSS Statistics Regression, SPSS Data Solution, 2013.
[30] P. Royston, Approximating the shapiro-wilk W-test for non-normality, Stat. Comput. 2 (3) (1992) 117–119.
[31] M.S. Srivastava, T.K. Hui, On assessing multivariate normality based on Shapiro-Wilk w statistic, Stat. Probab. Lett. 5 (1987) 15–18.
[32] J.F. Hair Jr., W.C. Black, B.J. Babin, R.E. Anderson, Multivariate Data Analysis, seventh ed., Prentice-Hall, 2009.
[33] M.R. Kianifar, F. Campean, Performance evaluation of metamodeling methods for engineering problems: towards a practitioner, Struct. Multidiscip. Optim. 61 (2020) 159–186.
[34] R. Huang, J. Ling, V. Aute, Comparison of approximation-assisted heat exchanger models for steady-state simulation of vapor compression system, Appl. Therm. Eng. 166 (2020) 114691.
[35] D. You, D. Liu, X. Jiang, X. Cheng, X. Wang, Temperature uncertainty analysis of injection mechanism based on kriging modelling, Mater 10 (11) (2017) 1319.
[36] T.H. Lee, J.J. Jung, Kriging metamodel based optimization, Optim. Struct. Mech. Syst. (2007) 445–484.
[37] K.T. Fang, R. Li, A. Sudjianto, Design and Modeling for Computer Experiments, first ed., Chapman & Hall/CRC, Boca Raton, FL, USA, 2006.
[38] J.H. Anthony, Probability and Statistics for Engineers and Scientist, fourth ed., THOMSON BROOKS/COLES, 2012.